Surface properties of cork: Is cork a hydrophobic material?

Julie Chanut, Yiqian Wang, Irene Dal Cin, Eric Ferret, Régis Gougeon, Jean-Pierre Bellat, Thomas Karbowiak

Version of Record: https://www.sciencedirect.com/science/article/pii/S002197972101599X
Manuscript_949717d95bf282f9b5ef6a47b9bc540d

Surface properties of cork:

Is cork a hydrophobic material?

Julie Chanut [a,b], Yiqian Wang [a], Irene Dal Cin [a], Eric Ferret [a], Régis D. Gougeon [a,c], Jean-Pierre Bellat [b], Thomas Karbowiak [a,*]

[a] Univ. Bourgogne Franche-Comté, AgroSup Dijon, PAM UMR 02 102, 1 Esplanade Erasme, 21000 Dijon, France.

[b] Univ. Bourgogne Franche-Comté, Laboratoire Interdisciplinaire Carnot de Bourgogne, UMR 6303 CNRS, 9 Avenue Alain Savary, 21078 Dijon, France.

[c] Univ. Bourgogne Franche-Comté, Institut Universitaire de la Vigne et du Vin, 1 rue Claude Ladrey, 21000 Dijon, France.

Email adress :
julie.chanut@agrosupdijon.fr
yiqian.wang@agrosupdijon.fr
irene.dal@studenti.unimi.it
eric.ferret@agrosupdijon.fr
regis.gougeon@u-bourgogne.fr
jean-pierre.bellat@u-bourgogne.fr

[*] Corresponding Author:

Prof. Thomas Karbowiak, Univ. Bourgogne Franche-Comté, AgroSup Dijon, PAM UMR 02 102, 1 Esplanade Erasme, 21000 Dijon, France,

phone number: +33380772388,

e-mail : thomas.karbowiak@agrosupdijon.fr

Abstract

Knowledge of the surface tension of cork and its hydrophobicity is of critical importance in many applications of this material at the interface with solid or liquid phases. The conventional technique based on contact angle measurement by sessile drop is not adapted to this naturally textured material and does not allow to accurately determine its hydrophobic character. A study based on capillary rise measurement is reported. A statistical distribution of the surface tension of cork is obtained, based on experiments performed on cork powder with various liquids and using a specific data processing to take into account the intrinsic heterogeneity of cork. This gives a surface tension of 22.6 (± 1.2) $mN{\cdot}m^{-1}$, with a polar component at 5.2 (± 0.5) $mN{\cdot}m^{-1}$ and a dispersive component at 17.4 (± 1.6) $mN{\cdot}m^{-1}$. With a water contact angle of around 90°, cork shows an intermediate hydrophobic/hydrophilic behaviour. Locally, the specific surface texture and chemical composition can reinforce either the hydrophobic or the hydrophilic character. This critical analysis invites reflection on the notion of surface hydrophobicity as it can be determined macroscopically by a contact angle measurement and as defined at the molecular level by the free enthalpy of sorption of water.

Keywords: hydrophobicity, surface tension, contact angle, capillary rise, wettability, surface roughness

1. Introduction

Cork is a natural material produced from the phellogen tissue of *Quercus suber L*. [1-3]. This outer bark, composed of suberized dead and empty cells, acts as a protective barrier for the tree against dehydration and fire [4]. It is sprinkled with lenticels, which are lignified channels of millimetre-size diameter, ensuring gas exchange between the tree and the outer environment (Fig. 1A). Cork displays remarkable properties such as low density, low permeability to liquids and gases, chemical and biological inertia, good elasticity, high damping capacity and low thermal conductivity [3]. Thanks to these properties, cork has been extensively used both for traditional and emerging applications, whether in its natural form or as a composite material, made of cork particles and adhesives. With around 200, 000 tons harvested every year, cork is a material of everyday life. The main sector of cork products is the wine industry with more than 12 billion bottles sealed with cork per year. To a lesser extent, cork stoppers are used for spirits, beer, oil, and other beverages. For the manufacture of stoppers, 41 % of the cork production is used as natural cork and 32 % as agglomerated cork [5]. For non-food applications, 24 % of the cork production is dedicated to building materials in architecture, for thermal and acoustic insulation, wall and floor coverings [1, 4, 6]. Cork can also be found in design and fashion (badminton shuttlecock, helmet, shoe insoles…). High technology applications of cork have been more recently developed, such as activated carbon for pollutants sorption [7-9], or aerospace material owing to its slow burn rate and shock absorption capacity [4].

The popularity of cork is firstly inseparable from the physical properties conferred by its specific texture. Cork phellem displays a typical alveolar pattern, imparting a noticeable anisotropy. Its 3D structure has progressively been revealed using different imaging techniques [10, 11]. The geometry of phellem cells varies according to the observation plane (Fig. 1B). In the radial plane (plane perpendicular to the radial direction), cells appear as hexagons that are arranged with mostly a honeycomb structure (Fig. 1Biii). In the two other planes, either perpendicular to the tangential or axial directions, they exhibit a rectangular shape and are stacked like a brick wall (Fig. 1Bi and 1Bii). Based on scanning electron microscopy (SEM) observations, the characteristic thickness of the cell wall is around 1 µm, the length of the hexagon edges 20 µm and the height of the cell 40 µm (Fig. 1C) [2, 10, 11]. However, cork cell size depends on climate conditions and on the annual biological rhythm, leading to cork growth ring formation [2, 12, 13]. Earlycork cells are greater in height and have thinner cell walls, while latecork cells are smaller and display a thicker wall [1].

Moreover, the chemical composition of cork is also an important factor influencing its properties [3, 10]. Cork is essentially composed of suberin (33-62 wt %), lignin (13-29 wt %) and polysaccharides (6-26 wt %). Extractable substances (e.g. tannin, glycerin) and mineral components (e.g. potassium, sodium), account for a smaller fraction of the cork chemical composition (8-24 wt %) (Fig. 1D) [4, 14]. The proportion of these constituents varies according to many parameters such as geographical origin, morphological location on the tree, age, production area and climate conditions [4, 7, 15]. Furthermore, differences can also be observed in the chemical composition between the cells of the phellem and those bordering the lenticels. The cell walls at the boundary of the lenticels , derived from the lenticular differentiation of phellogen, are mainly composed of lignin, whereas the cell walls of phellem are mostly composed of suberin [11].

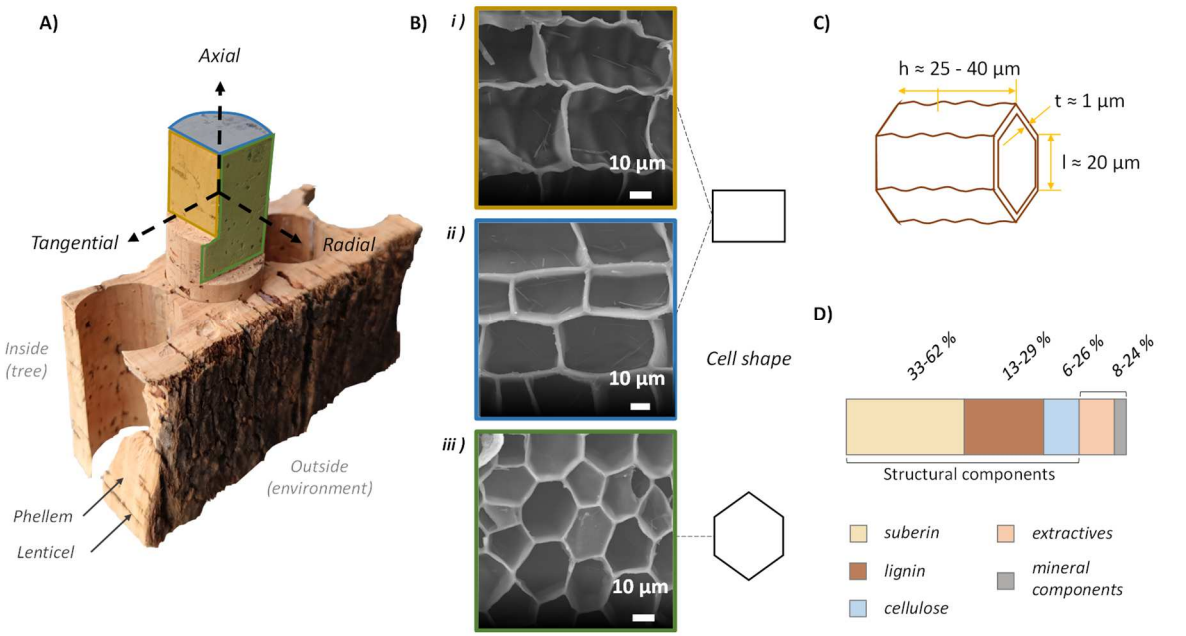

Figure 1: Characteristic physical structure and chemical composition of cork. A) Cork macroscopic structure illustrated by a punched bark with a stopper; B) Scanning Electron Microscopy observations from: (i) Tangential direction (or radial plane), (ii) Axial direction (or transverse plane) and (iii) Radial direction (or tangential plane); C) Characteristic shape and dimension of a cork cell (adapted from Gibson et al.*[10]); D) Chemical composition of cork (in weight %) [4, 7, 15].*

Both the physical structure and chemical composition contribute to defining the surface properties of cork. Determination of the surface tension of cork is of outmost importance in many applications where cork interacts with other substances. [16-18] For example, agglomerates require good coating and adhesion between cork particles and glue. In the production of cork stoppers, a surface treatment is also applied to facilitate uncorking. This requires an optimal coating of the slippery agent on the surface. Wettability studies are based on the measurement of contact angle, which indicates the ability of a solid to form a common interface with a liquid. Low contact angles (< 90°) correspond to high wettability, whereas large contact angles (> 90°) indicate low wettability. The contact angle formed by a drop of liquid on a solid surface and surrounded by its vapor was first defined by Thomas Young, in 1805 [19], as the equilibrium of the drop under the action of three interfacial tensions, with the corresponding well-known equation (Eq.1):

$$\sigma_{SL} = \sigma_{SV} - \sigma_{LV} \cos\theta \quad (1)$$

where σ_{SV} is the surface tension of the solid (mN·m^{-1}), σ_{LV} is the surface tension of the liquid (mN·m^{-1}), σ_{SL} is the interfacial tension between solid and liquid (mN·m^{-1}) and θ is the contact angle (°). This equation applies to an ideal solid surface, which means smooth, rigid, insoluble, nonreactive, and

chemically homogeneous. According to Fowkes [20], surface tension can be described as the sum of the contributions from different intermolecular forces at the surface (Eq. 2):

$$\sigma = \sigma^p + \sigma^d \quad (2)$$

where σ^p is the polar component and σ^d the dispersive component of the surface tension. They both contribute to the interaction of cohesion between phases. On the one hand, the polar component comprises dipole-dipole interactions (or Keesom forces), dipole-induced dipole interactions (or Debye forces) and hydrogen bonds. On the other hand, the dispersive component consists of induced dipole-induced dipole interactions known as dispersion forces or London forces [20]. The knowledge of both the polar and dispersive components are essential to better understand the interaction of cork with other substances in order to optimize the adhesion and coating process of cork-based materials.

Although surface tension is a key parameter to assess, its determination for cork has revealed an extreme complexity due to the surface heterogeneity of the material [21-23]. Sessile drop contact angle measurement did not give reliable results to characterize polar and dispersive components [22, 23]. Two different studies reported a total surface tension of 18 (± 4) $mN{\cdot}m^{-1}$ and 32 (± 3) $mN{\cdot}m^{-1}$ at 24°C, with a polar component of 0 $mN{\cdot}m^{-1}$ and 8 $mN{\cdot}m^{-1}$, respectively [22, 23]. Inverse gas chromatography, which could be an interesting alternative method to avoid experimental limitation due to surface roughness, led to a higher value of 38 (± 1) $mN{\cdot}m^{-1}$, but which was only determined for the dispersive component at 40°C [24]. Notwithstanding that the results vary from one study to another; these measurements seem to indicate that cork is a rather hydrophobic material. Nevertheless, the real meaning of contact angle for such a rough and heterogeneous surface as cork can be difficult to establish. Both the specific texture and the chemical heterogeneity of the cork surface can influence the measurement. The aim of the present study is thus to deepen knowledge of the surface properties of cork and, more broadly, to show the possibility of investigating the surface properties of such heterogeneous materials by means of the capillary rise method.

2. Material and Methods

2.1. Cork

Raw natural cork originated from Portugal's Mora municipality. All experiments were performed on high-quality cork, without any washing or surface treatment. Cork stoppers are visually sorted into different categories according to their external appearance, mainly based on the lenticular porosity visible on their surface. They are classified from category 0 (or high quality cork) which presents the best visual aspect to category 6 which presents the weakest [25].

For contact angle measurement by goniometry using the sessile drop method, the samples were cut with a razor blade into 3-mm-thick slices, perpendicular to the axial direction, which corresponds to the transverse plane in contact with a drop of liquid.

For capillary rise measurement using tensiometry, the cork was manually powdered using a grinder and then sieved to obtain a powder with a particle size ranging between 0.50 mm and 0.71 mm in diameter (sieve Triplette & Renaud). Preliminary measurements performed with *n*-hexane, glycerol and water on cork particles having different sizes (0.25-0.50; 0.50-0.71; 0.71-1.0 mm diameter) gave similar values of surface tension. The intermediate size range (0.50-0.71 mm) was selected to deeply investigate the polar and dispersive components of the surface tension using five different liquids.

2.2. Liquids

The liquids used for determining the surface tension of cork are listed in Table 1, with their total surface tension (σ_L) as well as dispersive (σ_L^d) and polar (σ_L^p) components. They are sorted according to their $\sqrt{\sigma_L^p}/\sqrt{\sigma_L^d}$ value, from the least to the most polar liquid. The measurements were performed with *n*-hexane (≥97% purity, Sigma Aldrich), chloroform (extra pure, Riedel-de Haën), cyclopentanol (99% purity, Sigma Aldrich), glycerol (≥99.5% purity, Sigma Aldrich) and distilled water.

Table 1: Physico-chemical properties of the liquids used for surface tension measurement at 25°C.

Properties / Liquids	**Total surface tension** σ_L (mN·m^{-1})	**Dispersive component** σ_L^d (mN·m^{-1})	**Polar component** σ_L^p (mN·m^{-1})	***Reference***	**Density** ρ (g·cm^{-3})	***Reference***	**Viscosity** η (mPa·s)	***Reference***
*n-H*exane	18.4	18.4	0.0	*[26]*	0.7	*[27]*	0.3	*[27]*
Chloroform	27.5	25.9	1.6	*[28]*	1.5	*[29]*	0.6	*[30]*
Cyclopentanol	32.7	27.2	5.5	*[31]*	0.9	*[32]*	10.4	*[32]*
Glycerol	63.4	37.0	26.4	*[33]*	1.3	*[32]*	1412.0	*[34]*
Water	72.8	21.8	51.0	*[33]*	1.0	*[35]*	0.9	*[36]*

2.3. Goniometry: sessile drop method

The contact angle of water on the cork surface was measured by goniometry using the sessile drop method. Experiments were conducted under controlled temperature (25°C) and relative humidity (50%) conditions. A liquid drop of around 3 µL was deposited on the cork surface, paying particular attention to select a non-lenticel area. The contact angle was measured using a goniometer (DSA30, Krüss, Germany) equipped with an image analysis software (Advance, Drop Shape, version 1.9, Krüss, Germany). The duration of the experiment for each measurement was 60 seconds. As the value of the contact angle with water did not change with time, the average value was reported. Sixty repetitions were performed.

For the measurement of the advancing contact angle, a water drop of 3 µL was firstly deposited on the cork surface. Water was then added into the drop by 0.2 µL every second. The advancing contact angle θ_A corresponds to the contact angle measured right before the contact surface area increases with the addition of water. Secondly, for the measurement of the receding contact angle, the water was sucked out by 0.2 µL every second. The receding contact angle θ_R corresponds to the contact angle measured right before the contact surface area decreases with the removal of water. This procedure was repeated 10 times. The difference between θ_A and θ_R gives the wetting hysteresis, which depends on surface roughness.

2.4. Tensiometry: Washburn method

2.4.1. *Capillary rise measurement*

This method allows for the determination of the contact angle of a powder with a liquid, based on the capillary flow dynamics. First, 0.25g cork powder was filled into a glass tube (of 10 mm internal diameter and 50 mm height) and closed at the extremity with a cellulose filter. The powder was then compacted with a 500g cylinder for 10 seconds. Each sample was compacted with the same mass and duration. The glass tube was hung in a force tensiometer (K100, Krüss, Germany) equipped with a precision balance. When the liquid was brought into contact with the sample, it rose between the cork particles due to capillary forces. The mass of the migrating liquid was measured over time. The measurements were performed at 25°C. At least 5 repetitions were made for each liquid.

2.4.2. Calculation of the contact angle

The capillarity rise phenomenon can be described by the Washburn equation (Eq.3):

$$\frac{m^2}{t} = \frac{c \cdot \rho^2 \cdot \sigma_L \cdot cos\theta}{\eta} \qquad (3)$$

Where m is the mass of the migrating liquid (kg) at time t (s), η is the viscosity of the liquid (N·m^{-2}·s), ρ is the density of the liquid (kg·m^{-3}), θ is the contact angle (rad), σ_L is the surface tension of the liquid (N·m^{-1}) and c is the capillary constant of the powder (m^5). Firstly, using a fully wetting liquid as *n*-hexane, with a contact angle considered equal to 0, the mean value of the capillary constant *c* was determined. This constant is related to the geometrical characteristics of the sample bed used.

For this reason, the samples underwent the same compaction rate, as previously detailed in section 2.4.1. Five replicates were performed with *n*-hexane. The average value of the capillary constant obtained was 3.1 x 10^{-5} ± 0.5 x 10^{-5} cm^{-5}.

Secondly, this value of c was used in Equation 3 to obtain the contact angle θ of cork with each liquid from Table 1, calculated from the initial linear part of the slope of the $m^2 = f(t)$ plot. It is noteworthy that a contact angle greater than 90° cannot be measured using this method, as no wetting of the powder takes place. A specific program was developed (and detailed in section 2.6) to take into account the variability brought by each step of the measurement on the final calculation of the surface tension and including its polar and dispersive components.

2.5. Determination of the polar and dispersive components of the surface tension by the Owens and Wendt method

The surface tension of cork σ_S and its polar σ_S^p and dispersive σ_S^d components were determined using the Owens and Wendt method (Eq. 4) [37]:

$$\frac{\sigma_L\,(\cos\theta + 1)}{2\sqrt{\sigma_L^d}} = \sqrt{\sigma_S^p}\,.\sqrt{\frac{\sigma_L^p}{\sigma_L^d}} + \sqrt{\sigma_S^d} \qquad (4)$$

where θ is the contact angle, σ_L is the surface tension of the liquid, with σ_L^p its polar component and σ_L^d its dispersive component, and σ_S is the surface tension of the solid (cork) tested, with σ_S^p its polar component and σ_S^d its dispersive component. The contact angle is expressed in degrees and all the surface tension parameters are given in mN·m^{-1}. From the linear regression of $\frac{\sigma_L(1+cos\theta)}{2\sqrt{\sigma_L^d}}$ as a function of $\sqrt{\frac{\sigma_L^p}{\sigma_L^d}}$, the polar and dispersive component σ_S^p and σ_S^d of cork can be calculated.

2.6. Statistical analysis

A specific program has been developed on Matlab (MathWorks, R2018a) to take into account the variability induced both by experimental analysis and data treatment. This includes experimental variability on the determination of the capillary constant c with *n*-hexane (Eq. 3, with $\cos\theta = 1$), experimental variability on the determination of the contact angle value θ with each liquid (Eq. 3, with known constant c) and variability due to fitting the Owens and Wendt model to the experimental data θ (linear regression from Eq. 4, with previously determined θ values for each liquid).

p replicates were obtained experimentally for the constant c determined with *n*-hexane. q_i replicates were performed experimentally with each liquid i. *n*-hexane was obviously not included as a liquid, as it was already used for the determination of the constant c. This led to pq_i values of θ calculated for each liquid, and thus, combining all θ values with the constants c, to a total number of regressions of (Eq. 5):

$$n = \prod_i pq_i \qquad (5)$$

In our case, in addition to *n*-hexane, 4 liquids were used (chloroform, cyclopentanol, glycerol and water), with p= 5 and q_i = 6, 5, 6 and 5, respectively. This gave a total number of regressions of $n = 562,500$. The resulting Owens and Wendt plot is provided with the mean linear regression and standard deviation, corresponding to 95% of the distribution obtained from the n regressions. From Equation 4, the corresponding distributions for the values of the polar σ_S^p and dispersive σ_S^d components of cork were obtained. The mean values and respective standard deviations were extracted from these distributions.

2.7. Cork surface imaging

2.7.1. Scanning electron microscopy

Morphological characterization of cork, as powder or slice, was performed by SEM, using a Jeol JSM 7600F apparatus operating at 5 kV. Prior to analysis, cork samples were coated with carbon (15–20 nm).

2.7.2. Two-photon microscopy

Two-photon microscopy was used to visualize the behaviour of water on the surface of cork. Observation of the cell structure of cork is based on the autofluorescence of lignin and suberin, which displays a range of emission from 440 to 540 nm and from 460 to 500 nm, respectively. Prior to observation, water was coloured with 10 nM rhodamine, which displays a maximum emission at 572 nm, giving a red/orange colour. Images were collected on a Nikon A1-MP scanning microscope equipped with a Plan APO IR 60x objective (NA, 1.27; Water Immersion, Nikon) at a scanning speed of 1 frame·s^{-1}. An IR laser (Chameleon, Coherent) was used to provide excitation at 800 nm. The fluorescence emission was collected on four detection channels: FF01-492/SP (400–492 nm),

FF03525/50 (500–550 nm), FF01-575/25 (563–588 nm) and FF01-629/56 (601–657 nm) (Semrock). Images were obtained by merging these four detection channels without any other spectral selection. Observation was performed along the plane perpendicular to the axial direction of cork, scanning over approximately 50 µm from water deposited on cork down to the first layer of cork cells below the surface.

3. Results and discussion

3.1. Physical and chemical heterogeneity of the cork surface

First, the surface hydrophobicity of cork was evaluated using the most classical technique, determining the contact angle formed between a drop of water and the cork surface (Fig. 2A). The experimental contact angle values and corresponding statistical distribution are displayed in Figure 2B. They cover a wide range from 60° to 140°. This gives a questionable average contact angle value of about 101° (± 18°), even if determined on 60 replicates and on the non-lenticel area only. Such variability obviously covers the few values already reported in the literature, using the same method. Abenojar *et al.* obtained water contact angle values between 90° and 100° from triplicate measurements at 24°C [22]. Gomes *et al*. determined an average contact angle of 84° on 20 replicates, in the range from 70° to 95°, at 24°C [23]. This broad distribution of contact angle values can be attributed to variations in the chemical composition and the texture of cork. Indeed, in the case of earlycork cells, a volume of 1 cm^3 of cork can contain 40 to 70 million of cells. For latecork cells, this number increases to 100 to 200 million of cells per cubic centimetre [3]. The greater dispersion of contact angle values observed in our study may also be due to the region of the cork surface analysed. The water drop was deposited randomly over the sample surface (excluding areas with lenticels), whereas in their study, Gomes *et al.* selected a narrower region, corresponding to the second growth ring, with the largest cork cells.

In support of the sessile drop analysis of water contact angle, advancing (θ_A) and receding (θ_R) contact angles measurements were also considered. The resulting wetting hysteresis is related to the surface roughness [38]. This is observed on almost all real surfaces. The contact angle formed by a liquid advancing on an unwetted surface is generally greater than the contact angle of the same liquid receding on a wetted surface, leading to a positive hysteresis ($\theta_A > \theta_R$). This indicates a complete or partial residual wetting of the solid surface by the liquid. On the cork surface, both advancing and receding values were very difficult to determine. Advancing contact angle gave variable results as previously discussed. Considering the highest contact angle values, close to a superhydrophobic state, a fakir effect might be expected on such a textured surface as cork. However, surprisingly, in the case of receding contact angle, as water was gradually removed from the drop, no decrease in the contact area between the water drop and the cork surface was noticeable. It is thus impossible to determine any θ_R value and a fortiori any hysteresis linked to the roughness of the cork surface. This wetting phenomenon could be attributed to a filling of the open cork cells present on the surface by water.

To better understand the behaviour of water with the cork surface, a visual experiment based on two-photon microscopy was performed (Fig. 2C). In this figure, the cork cells appear with a blue-green colour, while the water is coloured orange/red. Cork surface was observed to a depth of 50 µm, from the water layer on the cork surface down to the bottom of the first layer of cork cells. Figure 2C shows the images scanned along the depth of the sample (z-axis) along the plane perpendicular to the axial direction of the cork. The orange fluorochrome from water remains visible until the bottom of the cork cell (Fig. 2Cvi). These observations highlight that water completely fills the cork cell cavity. This was observed for most of the open cells from the cork surface. This is in agreement with the previous receding contact angle measurements in which the water seemed to remain stuck in the open cells present on the cork surface to form a covering film that is then impossible to remove.

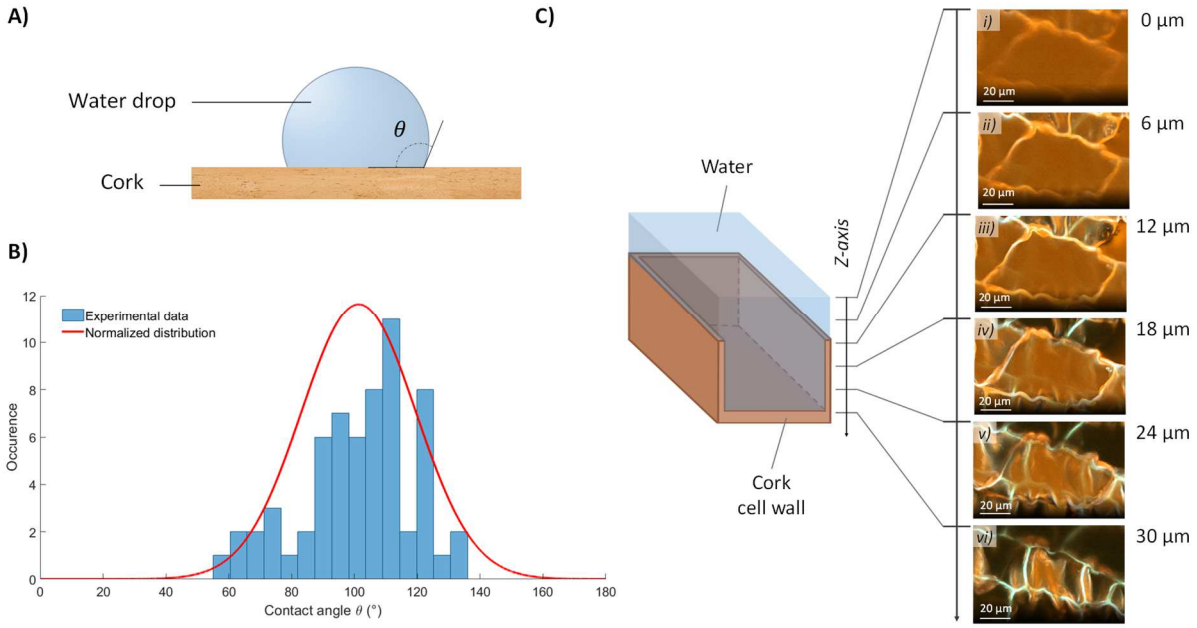

Figure 2: Water on the cork surface.
A) Schematic illustration of sessile drop measurement applied on cork; B) Distribution of water contact angle as determined on the cork surface from the sessile drop measurements (blue bars: experimental data, red line: normalized distribution); C) Two-photon microscopy observations of a cork cell from the surface in contact with water viewed along the axial direction.

Therefore, the sessile drop method does not seem to be appropriate for determining any contact angle on such a textured surface as cork. A noticeable discrepancy appears between contact angle measurements and microscopy observations. Direct measurement of the contact angle of cork with water, displaying an average value greater than 90°, would tend toward a rather hydrophobic material with little interaction with water, while two-photon microscopy observation shows a rather good interaction of cork with water, which fills most of the open cork cells present on the surface. To overcome the limitations due to surface roughness of cork, small-scale contact angle measurements on a single cork cell were attempted. However, the smallest droplet volume that could be deposited, in the order of 30 picolitres, gave a base surface area still larger than the surface area of a single cork cell. As it was not possible to get rid of the surface roughness, another approach was then considered.

Indeed, applying capillary rise measurements to cork particles allowed for a considerable increase in the surface of cork in contact with the liquid, and thus consideration of both the physical and chemical heterogeneity of the material. In particular, the lenticel regions can contribute to the hydrophilic character, as reported in our previous study on water sorption [39].

3.2. Determination of cork surface tension

The surface tension of cork was critically assessed by the Washburn capillary rise method, using calibrated cork particles (Fig. 3A). Prior to experiments, SEM observation revealed that the cork particles, ranging in size between 0.50 and 0.71 mm, did not show the specific orientation of the cells (Fig. 3B). The surface of the particles is mostly composed of open cells with edges that have been slightly abraded during the grinding process.

Hexane was first used for capillary rise owing to its ability to fully wet cork powder in a short time [17]. This allowed for evaluation of the c constant of the Washburn equation (Eq. 3). Then, from the slope of the linear part of the $m^2 = f(t)$ plot, the contact angle values for the different liquids listed in Table 1 were determined. The duration of the experiment ranged from a few seconds to several hours, depending on the liquid. The respective values of the contact angles are 42.5° (± 3.5°) for chloroform, 45.2° (± 6.8°) for cyclopentanol and 81.5° (± 2.3°) for glycerol. In the case of water, a smaller contact angle than that measured by the sessile drop was obtained with a value of 89.9° (± 0.1°). It is noteworthy that, with an angle of 90°, although it comes rather close to the limit of the method, a migration front of water was clearly detected with a slow progression rate (about 100 mg in a few hours).

The results obtained for each liquid are fairly reproducible compared with the previous distribution obtained from the sessile drop method. This can be ascribed to the large contact surface offered by the cork to liquid during the capillary rise flow. In the sessile drop method, the contact area between the cork and the liquid drop is around 7 mm^2, which corresponds to a maximum of 9,000 cork cells. In the case of the capillary rise method, it is increased to around 1.1 x 10 ^{4} mm^2, which means up to 1.25 x 10^7 cork cells. Thus, such a large contact surface area allows for taking into consideration the heterogeneity originating both from the chemical composition and from the texture of the material. Indeed, cork powder contained non-sorted particles comprising a representative mixture of the original material with earlycork cells, latecork cells and cells forming the border of the lenticels. Besides, the anisotropy of the material is also smoothed out, since all three orientations of the cork cells are represented in the considered sample.

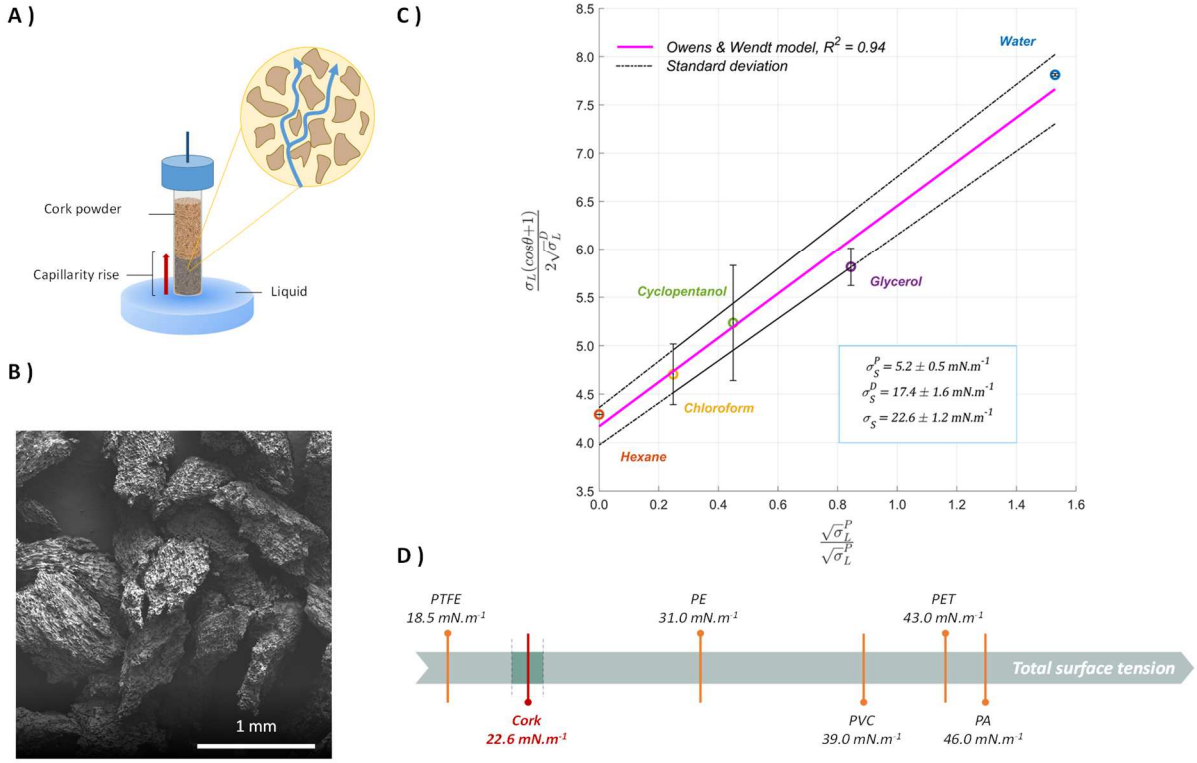

Figure 3: Surface tension of cork.

A) Principle of the Washburn capillary rise measurement applied on cork powder; B) Scanning Electron Microscopy observation of the cork particles; C) Owens and Wendt plot for determining the dispersive and polar components of the surface tension of cork, included the variability related to experimental data and modelling; D) Surface tension of cork compared with some classical synthetic materials (values taken from [37]) (PTFE: Polytetrafluoroethylene, PE: Polyethylene, PVC: Polyvinylchloride, PET: Polyethylene terephthalate, PA: Polyamide).

The surface tension of the cork powder was then determined using the Owens and Wendt method (Eq. 4) thanks to a procedure detailed in section 2.6. Applying this statistical treatment allows for taking into account the three sources of the variability: (i) the experimental distributions in the values of the constant *c*; (ii) the experimental distributions in the values of each contact angle; and (iii) the variability resulting from the fitting of the Owens and Wendt model to experimental data. This global variability due to the cork heterogeneity and to the analytical procedure used is integrated in the final Owens and Wendt plot, as shown in Figure 3C. The surface tension of the cork powder, with polar and dispersive components, is calculated based on this modelling. The total surface tension of cork is 22.6 (± 1.2) $mN \cdot m^{-1}$, with a polar component at 5.2 (± 0.5) $mN \cdot m^{-1}$ and a dispersive component at 17.4 (± 1.6) $mN \cdot m^{-1}$.

3.3. Critical discussion about cork surface tension

In Figure 3D, the surface tension of cork is compared with that of conventional synthetic polymers at 25°C [37]. With a value of 22.6 $mN \cdot m^{-1}$, cork surface tension is surprisingly close to that of polytetrafluoroethylene (PTFE). It is also lower than the surface tension of most selected polymers. Thus, according to this parameter, cork falls into the category of low surface tension materials, with a value below 50 $mN \cdot m^{-1}$ [40].

Although such a result might suggest that cork is as hydrophobic as PTFE, other criteria must be critically examined. Firstly, the contact angle of water with cork (90°) is lower than that of PTFE (close to 114° [41]). It may be noticed that this contact angle, which is measured on a macroscopic scale by capillary rise, is obviously an apparent contact angle. It does not represent the true water contact angle that could be obtained at the surface of a single cell. It includes the surface roughness and the heterogeneity of the chemical composition of cork. Secondly, the polar component of the cork surface tension is of 5.2 $mN \cdot m^{-1}$, which accounts for 25% of the total surface tension. Thirdly, the sorption capacity of water on cork reaches a rather high content of around 9% (w/w), at 25°C and close to 90% relative humidity, as determined in our previous work [39]. Moreover, the energy of interaction between water and cork, measured by calorimetry, is around 65 $kJ \cdot mol^{-1}$ which is higher than the liquefaction enthalpy of 44 $kJ \cdot mol^{-1}$ [39]. This value is considerably higher than the 2.5 $kJ \cdot mol^{-1}$ reported for low surface tension materials [40]. This indicates that water molecules are sorbed on hydrophilic sites present on the cork surface. These could correspond to hydrophilic groups such as hydroxyls and methoxyls, which are known to be strong sorption sites for polar water molecules [39]. In addition, considering the entropic contributions of water sorption on cork [39], this gives a free enthalpy of sorption, so called Gibbs energy of sorption, which is around -22 $kJ \cdot mol^{-1}$ at 298 K. Compared to the free enthalpy of liquefaction of water (-8.5 $kJ \cdot mol^{-1}$ at 298 K), this means that cork displays a high affinity for water. Thus, cork appears to be a less hydrophobic material than initially suggested by the surface tension measurement using the capillary rise method.

In fact, the cork presents an intermediate behaviour. Its hydrophobic/hydrophilic character depends on the scale probed by the analytical method used. At the molecular level, it can be considered as a hydrophilic material owing to the rather high water/cork energy of interaction. By contrast, at the macroscopic level, with a low surface tension and a water contact angle around 90°, it appears as a rather hydrophobic material. The fact that cork appears at the macroscopic level as a more hydrophobic material than it actually is, comes from its specific honeycomb texture and the roughness conferred by the cell walls (Fig.2C).

Finally, this invites us to reconsider the notion of hydrophobicity of a material. In most cases, hydrophobicity is generally defined by considering the wetting behaviour of the surface with water, expressed as the value of the contact angle with water. Since hydrophobicity is related to the interaction of water with a surface, it can also be described by the free enthalpy of sorption, so called Gibbs energy of sorption [42]. When the free enthalpy of the water sorption is lower than the free enthalpy of water liquefaction, the surface is hydrophobic. When it is equivalent or higher, the surface is hydrophilic. In the case of cork, despite a contact angle with water close to 90° and a low surface tension, the free enthalpy of sorption shows that it is also capable of establishing interactions with water.

Conclusions

The surface tension of the cork and its wettability with water were assessed. First, the sessile drop method was performed with water on the cork surface, leading to an average value of around 100°, with a broad distribution. Although this may correspond to a rather hydrophobic material, this method is not suitable for a surface as textured and heterogeneous as cork. Another approach, the capillary rise method, was then used on cork particles, allowing for a considerable increase in the contact surface between the liquid and the cork particles. Thanks to specific data processing, the variability resulting from both the heterogeneity of the chemical composition and the physical texture of the material was thus taken into account. This led to a contact angle with water close to 90° and a surface tension of 22.6 (± 1.2) $mN{\cdot}m^{-1}$, with a polar component at 5.2 (± 0.5) $mN{\cdot}m^{-1}$ and a dispersive component at 17.4 (± 1.6) $mN{\cdot}m^{-1}$.

Such results might suggest that cork is a hydrophobic material. However, the polar component of the surface tension as well as the water sorption capacity and energy reveal that the cork has hydrophilic sites on its surface. The hydrophilic/hydrophobic behaviour thus depends on the scale probed. At the molecular scale, cork appears as a rather hydrophilic material whereas at the macroscopic scale, it can be considered a hydrophobic material.

The original approach proposed in this work allowed to question the values presented hitherto in the literature [23]. Furthermore, this critical analysis of the contribution of surface physics and chemistry to the hydrophobicity of a material invites reflection on the notion of surface hydrophobicity, as it can be determined macroscopically by contact angle measurement and is defined at the molecular scale by the free enthalpy of sorption of water [42].

The present work provides advanced knowledge on the surface properties of cork which will clearly be valuable for future applications. In particular, this opens up new perspectives to better understand the wetting phenomena of cork by liquids. For instance, this is of paramount importance in the elaboration of agglomerated cork-based materials with polyurethane adhesives, in the field of building materials or wine stoppers. For the latter, the control of the coating at the interface between cork and glass bottleneck is also a key parameter which requires a thorough understanding of the surface properties [43]. Lastly, the capillary rise method with a statistical processing appears to be a relevant tool in order to assess the surface properties of materials with high chemical and/or physical heterogeneity.

Acknowledgments

We would like to thank Diam Bouchage as well as the French National Association of Research and Technology (ANRT) for their financial support and Julie Chanut's PhD grant. Two-photon images were performed at Dimacell platform with the help of Pascale Winckler. The authors would also like to thank Frederic Herbst (Laboratoire Interdisciplinaire Carnot de Bourgogne) for MEB imaging and the DIVVA platform for the access to the equipment. The authors also thank Theeraphorn Panrong for her help during the experiments.

References

1. H. Pereira, M. E. Rosa and M. A. Fortes, The Cellular Structure of Cork from Quercus Suber L., IAWA Journal 8 (3) (1987) 213-218, https://doi.org/10.1163/22941932-90001048
2. A. Lagorce-Tachon, F. Mairesse, T. Karbowiak, R. D. Gougeon, J.-P. Bellat, T. Sliwa and J.-M. Simon, Contribution of image processing for analyzing the cellular structure of cork, Journal of Chemometrics 32 (1) (2018) 2988, https://doi.org/10.1002/cem.2988
3. H. Pereira, Cork: Biology, Production and Uses, (2007)
4. S. P. Silva, M. A. Sabino, E. M. Fernandes, V. M. Correlo, L. F. Boesel and R. L. Reis, Cork: properties, capabilities and applications, International Materials Reviews 6 (2005) 345-365, https://doi.org/10.1179/174328005X41168
5. APCOR, Cork Yearbook 2020, (2020)
6. G. E. Reiber, D. G. Smith, C. Wallace, K. Sullivan, S. Hayes, C. Vath, M. L. Maciejewski, O. Yu, P. J. Heagerty and J. LeMaster, Effect of therapeutic footwear on foot reulceration in patients with diabetes: a randomized controlled trial, Jama 287 (19) (2002) 2552-8, https://doi.org/10.1001/jama.287.19.2552
7. A. M. A. Pintor, C. I. A. Ferreira, J. C. Pereira, P. Correia, S. P. Silva, V. J. P. Vilar, C. M. S. Botelho and R. A. R. Boaventura, Use of cork powder and granules for the adsorption of pollutants: A review, Water Research 46 (10) (2012) 3152-3166, https://doi.org/10.1016/j.watres.2012.03.048
8. A. P. Carvalho, M. Gomes, A. S. Mestre, J. Pires and M. B. d. Carvalho, Activated carbons from cork waste by chemicalactivation with K2CO3 Application to adsorption of natural gas components, Carbon 42 (2004) 667–691, https://doi.org/10.1016/j.carbon.2003.12.075
9. N. Chubar, J. R. Carvalho and M. J. N. Correia, Heavy metals biosorption on cork biomass: effect of the pre-treatment, Colloids and Surfaces A: Physicochemical and Engineering Aspects 238 (1) (2004) 51-58, https://doi.org/10.1016/j.colsurfa.2004.01.039
10. L. J. Gibson, K. E. Easterling and M. F. Ashby, The structure and mechanics of cork Proceedings of the Royal Society of London 377 (A) (1981) 99-117, https://doi.org/10.1098/rspa.1981.0117
11. K. Crouvisier-Urion, J. Chanut, A. Lagorce, P. Winckler, Z. Wang, P. Verboven, B. Nicolai, J. Lherminier, E. Ferret, R. D. Gougeon, J.-P. Bellat and T. Karbowiak, Four hundred years of cork imaging: New advances in the characterization of the cork structure, Scientific Reports 9 (1) (2019) 19682, https://doi.org/10.1038/s41598-019-55193-9
12. A. Costa, H. Pereira and Â. Oliveira, Influence of climate on the seasonality of radial growth of cork oak during a cork production cycle, Annals of Forest Science 59 (4) (2002) 429-437, https://doi.org/10.1051/forest:2002017
13. G. Oliveira, M. A. Martins-Loução and O. Correia, The relative importance of cork harvesting and climate for stem radial growth of Quercus suber L, Annals of Forest Science 59 (4) (2002) 439-443, https://doi.org/10.1051/forest:2002018
14. R. T. Teixeira and H. Pereira, Suberized cell walls of cork from cork oak differ from other species, Microscopy and Microanalysis 16 (5) (2010) 569-75, https://doi.org/10.1017/s1431927610093839
15. H. Pereira, Chemical composition and variability of cork from Quercus suber L, Wood Science and Technology 22 (3) (1988) 211-218, https://doi.org/10.1007/BF00386015
16. M. Joao Teixeira, A. C. Fernandes, B. Saramago, M. E. Rosa and J. C. Bordado, Influence of the wetting properties of polymeric adhesives on the mechanical behaviour of cork agglomerates, Journal

of Adhesion Science and Technology 10 (11) (1996) 1111-1127, https://doi.org/10.1163/156856196X00148
17. S. P. Magalhães da Silva and J. M. Oliveira, Cork powders wettability by the Washburn capillary rise method, Powder Technology 387 (2021) 16-21, https://doi.org/10.1016/j.powtec.2021.04.005
18. T. Karbowiak, F. Debeaufort and A. Voilley, Importance of Surface Tension Characterization for Food, Pharmaceutical and Packaging Products: A Review, Critical Reviews in Food Science and Nutrition 46 (5) (2006) 391-407, https://doi.org/10.1080/10408390591000884
19. T. Young, III. An essay on the cohesion of fluids, Philosophical Transactions of the Royal Society of London 95 (1805) 65-87, https://doi.org/10.1098/rstl.1805.0005
20. F. M. Fowkes, Attractive forces at interfaces, Industrial & Engineering Chemistry 56 (12) (1964) 40-52, https://doi.org/10.1021/ie50660a008
21. F. B. Abdallah, R. B. Cheikh, M. Baklouti, Z. Denchev and A. M. Cunha, Effect of surface treatment in cork reinforced composites, Journal of Polymer Research 17 (2009) 519-528, https://doi.org/10.1007/s10965-009-9339-y
22. J. Abenojar, A. Q. Barbosa, Y. Ballesteros, J. C. d. Real, L. F. M. d. Silva and M. A. Martinez, Effect of surface treatments on natural cork: surface energy, adhesion, and acoustic insulation, Wood Science Technology 48 (2013) 207-224, https://doi.org/10.1007/s00226-013-0599-7
23. C. M. C. P. S. Gomes, A. C. Fernandes and B. d. J. V. S. Almeida, The Surface Tension of Cork from Contact Angle Measurements, Journal of Colloid and Interface Science 156 (1) (1993) 195-201, https://doi.org/10.1006/jcis.1993.1099
24. N. Cordeiro, C. P. Neto, A. Gandini and M. N. Belgacem, Characterization of the Cork Surface by Inverse Gas Chromatography, Journal of Colloid and Interface Science 174 (1) (1995) 246-249, https://doi.org/10.1006/jcis.1995.1387
25. A. Lefebvre, J.-M. Riboulet, C. Alegoet, C. Pouillaude, F. Lacorne and J. V. Natividade, Charte des bouchonniers liègeurs, (2006)
26. J. Schultz, K. Tsutsumi and J.-B. Donnet, Surface properties of high-energy solids: I. Determination of the dispersive component of the surface free energy of mica and its energy of adhesion to water and n-alkanes, Journal of Colloid and Interface Science 59 (2) (1977) 272-276, https://doi.org/10.1016/0021-9797(77)90008-X
27. A. Sharma, M. Rani and S. Maken, Thermodynamics of haloarenes with n-hexane at 298.15–318.15 K: Density, ultrasonic speed and viscosity, Journal of Molecular Liquids (2020) 114366, https://doi.org/10.1016/j.molliq.2020.114366
28. J. Schultz, K. Tsutsumi and J.-B. Donnet, Surface properties of high-energy solids: II. Determination of the nondispersive component of the surface free energy of mica and its energy of adhesion to polar liquids, Journal of Colloid and Interface Science 59 (2) (1977) 277-282, https://doi.org/10.1016/0021-9797(77)90009-1
29. W. M. Haynes, CRC Handbook of Chemistry and Physics, 95th Edition, (2014-2015)
30. J. Speight, Lange's Handbook of Chemistry, 16th Edition, (2005)
31. K. F. Gebhardt, Grundlagen der physikalischen Chemie von Grenzflächen und Methoden zur Bestimmung grenzflächenenergetischer Größen, (1982)
32. D. R. Lide, CRC Handbook of Chemistry and Physics, 88th Edition, (2007-2008)
33. G. Ström, M. Fredriksson and P. Stenius, Contact angles, work of adhesion, and interfacial tensions at a dissolving Hydrocarbon surface, Journal of Colloid and Interface Science 119 (2) (1987) 352-361, https://doi.org/10.1016/0021-9797(87)90280-3
34. J. B. Segur and H. E. Oberstar, Viscosity of Glycerol and Its Aqueous Solutions, Industrial & Engineering Chemistry 43 (9) (1951) 2117-2120, https://doi.org/10.1021/ie50501a040
35. M. J. O'Neil, The Merck Index: An Encyclopedia of Chemicals, Drugs, and Biologicals, 15th Edition, 74 (2013)
36. F. Van der Leeden, F. L. Troise and D. K. Todd, The Water Encyclopedia, 2nd edition (1990)
37. D. K. Owens and R. C. Wendt, Estimation of the surface free energy of polymers, Journal of Applied Polymer Science 13 (8) (1969) 1741-1747, https://doi.org/10.1002/app.1969.070130815

38. R. H. Dettre and R. E. Johnson, Contact Angle Hysteresis, 43 (1964) 136-144, https://doi.org/10.1021/ba-1964-0043.ch008
39. S. Lequin, D. Chassagne, T. Karbowiak, R. D. Gougeon, L. Brachais and J.-P. Bellat, Adsorption Equilibria of Water Vapor on Cork, Journal of Agricultural and Food Chemistry 58 (2010) 3438-3445, https://doi.org/10.1021/jf9039364
40. P.-G. d. Gennes, F. Brochard-Wyart and D. Quere, Capillarity and Wetting Phenomena. Drops, Bubbles, Pearls, Waves, 1, (2004) https://doi.org/10.1007/978-0-387-21656-0
41. M. K. Bernett and W. A. Zisman, Relation of Wettability by Aqueous Solutions to the Surface Constitution of Low-energy Solids, The Journal of Physical Chemistry 63 (8) (1959) 1241-1246, https://doi.org/10.1021/j150578a006
42. T. Karbowiak, G. Weber and J.-P. Bellat, Confinement of Water in Hydrophobic Nanopores: Effect of the Geometry on the Energy of Intrusion, Langmuir 30 (1) (2014) 213-219, https://doi.org/10.1021/la4043183
43. J. Chanut, J.-P. Bellat, R. D. Gougeon and T. Karbowiak, Controlled diffusion by thin layer coating: The intricate case of the glass-stopper interface, Food Control 120 (2021) 107446, https://doi.org/10.1016/j.foodcont.2020.107446

Figure 1: Characteristic physical structure and chemical composition of cork. A) Cork macroscopic structure illustrated by a punched bark with a stopper; B) Scanning Electron Microscopy observations from: (i) Tangential direction (or radial plane), (ii) Axial direction (or transverse plane) and (iii) Radial direction (or tangential plane); C) Characteristic shape and dimension of a cork cell (adapted from Gibson et al. [10]); D) Chemical composition of cork (in weight %) [4, 7, 15].

Figure 2: Water on the cork surface. A) Schematic illustration of sessile drop measurement applied on cork; B) Distribution of water contact angle as determined on the cork surface from the sessile drop measurements (blue bars: experimental data, red line: normalized distribution); C) Two-photon microscopy observations of a cork cell from the surface in contact with water viewed along the axial direction.

Figure 3: Surface tension of cork. A) Principle of the Washburn capillary rise measurement applied on cork powder; B) Scanning Electron Microscopy observation of the cork particles; C) Owens and Wendt plot for determining the dispersive and polar components of the surface tension of cork, included the variability related to experimental data and modelling; D) Surface tension of cork compared with some classical synthetic materials (values taken from [37]) (PTFE: Polytetrafluoroethylene, PE: Polyethylene, PVC: Polyvinylchloride, PET: Polyethylene terephthalate, PA: Polyamide).

Table 1: Physico-chemical properties of the liquids used for surface tension measurement at 25°C.

Properties / **Liquids**	**Total surface tension** σ_L (mN·m^{-1})	**Dispersive component** σ_L^d (mN·m^{-1})	**Polar component** σ_L^p (mN·m^{-1})	***Reference***	**Density** ρ (g·cm^{-3})	***Reference***	**Viscosity** η (mPa·s)	***Reference***
*n-H*exane	18.4	18.4	0.0	*[26]*	0.7	*[27]*	0.3	*[27]*
Chloroform	27.5	25.9	1.6	*[28]*	1.5	*[29]*	0.6	*[30]*
Cyclopentanol	32.7	27.2	5.5	*[31]*	0.9	*[32]*	10.4	*[32]*
Glycerol	63.4	37.0	26.4	*[33]*	1.3	*[32]*	1412.0	*[34]*
Water	72.8	21.8	51.0	*[33]*	1.0	*[35]*	0.9	*[36]*

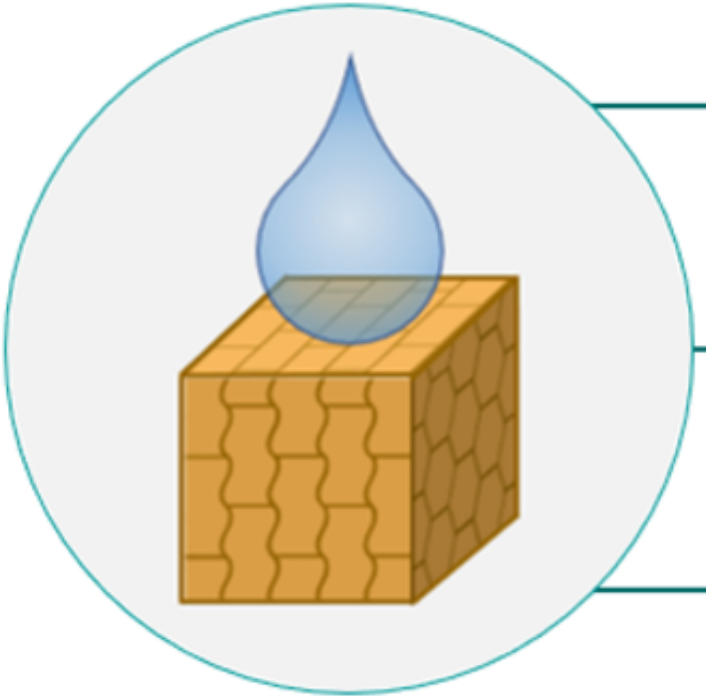

Physical structure

Chemical composition

Scale considered

Hydrophobicity?